Terahertz radiation from pentacene organic diode at room temperature

Jian Deng (邓 剑)[1,2], Yan Wang (王 艳)[1*], Bing Yang (杨 兵)[2], and Yuguang Ma (马於光)[2]**

[1]*College of Chemistry, Jilin University, Changchun 130012, China*
[2]*State Key Laboratory of Supramolecular Structure and Materials, Jilin University, Changchun 130012, China*
[*]*Corresponding author: wangy2011@jlu.edu.cn;* [**]*corresponding author: ygma@jlu.edu.cn*
Received September 3, 2014; October 24 2014; posted online December 29, 2014

We investigate terahertz radiation (T-rays) from a pentacene organic diode at room temperature. The quantum chemistry calculation for frequency-related Huang–Rhys factor of pentacene is also carried out. The results demonstrate that the T-rays can come from a bending vibration of pentacene skeleton after the energy of pentacene exciton transferring to the vibrational excited state via electron–phonon coupling. Frequency and natural bond orbital analytics of pentacene and its derivatives are performed in order to explain the result and develop new materials to get higher emission. This work provides a new way to produce T-rays with a simple device at room temperature.

OCIS codes: 230.0230, 250.0250, 310.0310.
doi: 10.3788/COL201513.012301.

Terahertz radiation (T-rays) with frequency between 10^{11} and 10^{13} Hz, and wavelength between 0.03 and 3 mm, is localized at the transition region from electronics to photonics, and from the microwave to infrared (IR) wave. Due to the T-rays spectrum's special sensitivity to molecular structures, it is especially useful for dynamic analysis and nondestructive detection in the safety check[1,2]. Currently, T-rays have attracted great deal of attention in both fundamental research and industrial applications[3–7]. T-rays can be generated by the interactions of ultrashort pulse laser with nonlinear optics crystal[8,9], or interactions of high-power laser with gas-like organic molecules such as methanol (CH_3OH) and ammonia (NH_3)[10,11]. However, bulky pumping laser equipments as well as low-energy conversion efficiency significantly restrict their wide application. T-rays based on quantum-cascade structures are portable and show high-energy conversion efficiency; yet, it must operate at very low temperature (typically 5 K) to achieve high efficiency at current stage[12,13]. Therefore, portable T-rays sources which can be operated at room temperature are highly desirable for the practical application.

As is well-known, there are many vibration modes in the organic molecule, and some of them, such as the puckering, breathing, and torsion motions of molecular skeleton, are located in the T-rays region (typically below 12 THz)[14]. Photophysical studies have shown that the electronic excited state sometimes can couple with this vibration state in some π-conjugated molecular systems, called as electron–phonon coupling, whose strength is relative to the Huang–Rhys factor[15]. Many π-conjugated molecules can emit fluorescence with high luminescent efficiency. However, in a strong vibration–excited state coupling system, the fluorescence is strongly quenched through the relaxation process vibrationally and rotationally[16–18]. Therefore, for the fluorescence materials, the electron–phonon coupling, which induces the non-irradiant process, is always a negative effect. As an inspiration, it may provide a new routine to transfer the energy from electronic excitation to vibration irradiation and get T-rays since many vibration modes of organic molecule are in the T-rays region, provided that there are enough electron–phonon coupling and appropriate IR activity. On the other hand, the π-conjugated molecules generally have the properties of semiconductor, their electronic excited state can be produced by recombination of injecting electron and hole in a device, such as an organic diode with sandwich structure. Therefore, if a π-conjugated molecule with strong vibration–excited state coupling is taken as a semiconductor to fabricate an organic diode, a large number of excited states can be formed when injected electron and hole recombine. And then the energy can be transferred from electronic excited states to vibration states of molecules to emit T-ray. The T-ray source from this way would be portable, compact, and easily operated at room temperature. This is our motivation to test the possibility of T-rays from the organic diode at room temperature.

From the analysis, the π-conjugated molecules with very low fluorescence efficiency but remarkable semiconductor properties should be chosen for our goal. As an original study, well-known semiconductor molecule pentacene is used for our experiments because of its high-carrier mobility (up to 35 cm^2/Vs in single crystal[19], and 0.1–0.8 cm^2/Vs in micro-crystalline film[20]), ambipolar properties[21,22], and no visible (Vis) fluorescence in solid form (Fig. 1). The high-carrier mobility indicates that enough excited states can be produced in pentacene

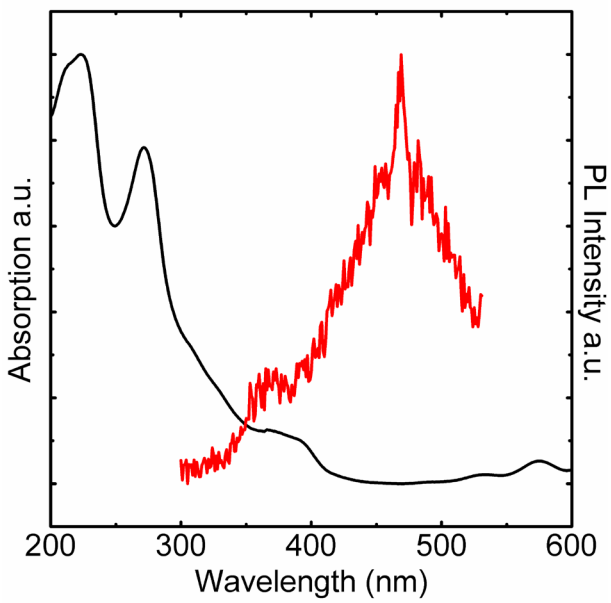

Fig. 1. UV-Vis absorption and fluorescence spectrum of pentacene film. The film was deposited by vacuum deposited on a quartz plate (pentacene film shows very weak emission).

film, and no Vis fluorescence indicates that fluorescence of pentacene may be strongly quenched by the strong vibration–excited state coupling. In order to inject electron and hole into pentacene, a device with the structure of Si/pentacene (80 nm)/LiF/Al was designed and fabricated (Fig. 2). P-Si was selected as anode because of its high transparency in T-rays window[23]. LiF/Al was used as cathode to inject electron effectively. The pentacene film was grown with a thickness of 80 nm by the vacuum deposition. Meanwhile, the quantum chemical calculation was used to test the possibility of getting THz from a pentacene molecule.

The p-Si (SI-500444, Niraco, resistivity ≤ 0.02 Ω cm) was cut by the size of 1.5×2.0 (cm), and then immersed into hydrofluoric aqua to remove the thin native SiO_2. The silicon was ultrasonically cleaned in deionized water, semiconductor lotion, deionized water, ethanol, acetone, toluene, acetone, and ethanol for three times successively. After 30 min IR irradiation and 20 min exposition to ultraviolet (UV) irradiation, the silicon

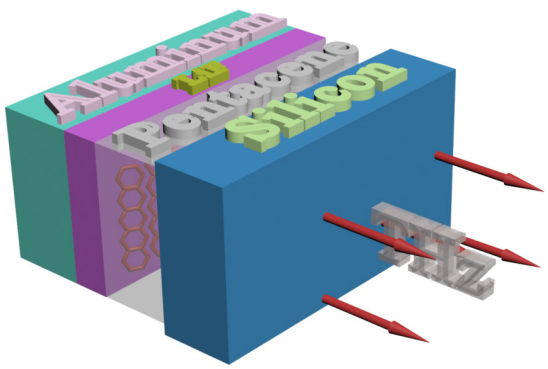

Fig. 2. Schematic illustration of device.

substrates were used to make the devices. Then pentacene (J&K, purity 98%) thin film was deposited on the substrates by vacuum evaporation with 80 nm thickness. During the deposition of pentacene, the pressure and the growth rate were kept $< 10^{-4}$ and 0.08 nm s^{-1}, respectively. At last, the 0.7 nm LiF and 150 nm Al (0.7×0.9 (cm)) was deposited by vacuum evaporation at a rate of 0.03 and 0.5 nm s^{-1}, respectively. In this letter, the estimated mobility of pentacene film was 0.1 cm^2/Vs. All the measurements were taken out at room temperature. The electric characters of these devices were studied by Keithley 2400 instrument. The THz radiation was monitored by a Bruker IFS 66v Fourier transform infrared (FTIR) spectroscopy.

The I–V curve of the device shows the typical diode characteristic (Fig. 3). The device exhibits the turn-on voltage at 2.5 V and current density as high as 159 mA/cm^2 at 4.2 V, reflecting high-carrier mobility and low injecting barrier of carriers both from cathode and anode in the pentacene device. As the driving voltage reached 2.5 V (current density is 29 mA/cm^2), a clear T-rays irradiation from this device was investigated by detector. The detected T-rays spectra were very sharp with the peak located at 78.6 cm^{-1} (2.36 THz) and the full-width at half-maximum (FWHM) of 0.35 THz. With the voltage increase from 2.5 to 3.5 V, the intensity of T-rays increased gradually. One can clearly observed that the T-rays frequency and FWHM almost did not change with voltage. When the applied voltage further increased, the intensity of T-rays dropped very fast, and almost no T-rays signal was detected from the devices as the applied voltage was higher than 5.5 V, which may result from the competition process between the electron–phonon coupling and direct electronic transition from exciton. In order to confirm the direct electronic transition process, the p-Si was replaced by UV-Vis transparency indium tin oxide (ITO) to fabricate devices. In the organic light-emitting diode (OLED) device with structure of ITO/pentacene (80 nm)/LiF/Al, by careful observation, a very weak red-light emitting was observed as device operation at driving voltage over 4.0 V. The weak red-light emission may come from the direct electronic transition. The same phenomenon will probably occur in the p-Si/pentacene (80 nm)/LiF/Al diode because of the similar structure. This competition process results in the fast drop of T-rays radiation at the high operation voltage.

The T-rays irradiation processes in the diode may be very complicated, whereas it seems reasonable as considering the possible relaxation routine of excitons. Usually, in the organic diodes, when the applied voltage is higher than turn-on voltage of device, the carriers (electrons and holes) can be injected into organic semiconductor from the electrodes, and exciton can be formed by the recombination of the injected electrons and holes. For the π-conjugated molecules with high fluorescent efficiency, the excitons will decay and emit

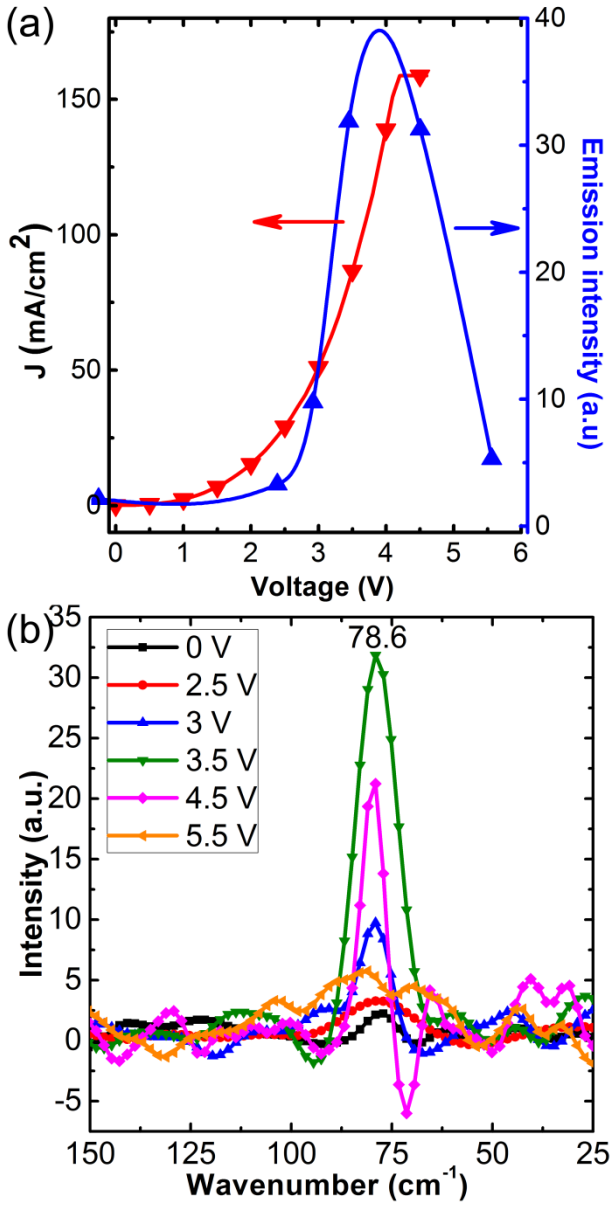

Fig. 3. Electric and T-rays radiation characteristic of pentacene devices based on organic-diode: (a) I–V characteristic and T-rays of devices and (b) T-rays from organic diode at room temperature in various voltages.

UV-Vis light directly via electronic transition. But if the materials used in the device have very low fluorescent efficiency, the energy of excitons will be consumed by various non-irradiation processes, such as internal conversion and intersystem crossing. In the case of very large spectral Stokes shift, the molecular excited state potential-energy curve crosses its ground state with high vibration levels, there will be a reorganization of its electronic state, switching from one state to another (the nuclear geometries of two states are the same at the crossing point). As a result, the energy of excitons can transfer to the vibration excited state via the electron–phonon coupling, and the vibration exciton energy can be relaxed by the vibration energy level transition with the generation of long-wavelength electromagnetic wave such as T-rays. The diagrammatic sketch of T-rays prototype is shown in Fig. 4. However, further experimental and theoretical works are needed to understand the mechanism.

Although the T-rays signal can be detected by the traditional FTIR detector, the conversion efficiency and output power is still relatively low. The Huang–Rhys factor is usually thought to be related to the strength of electron–phonon coupling. The larger the Huang–Rhys factor, the stronger the coupling is, which probably results in more efficient T-rays emission. In order to investigate the molecular structure-dependent electron–phonon coupling strength in the T-rays zone, some preliminary calculations of frequency-related Huang–Rhys factor is carried out on pentacene derivatives. In the calculation, the ground-state geometries were fully optimized using density functional theory (DFT) with B3LYP hybrid functional at the basis set level of 6–31G. The excited-state geometries were optimized by time-dependent DFT with B3LYP functional at the same basis set level. All the calculations were performed using Gaussian 09 package in PowerLeader workstation[24]. The normal mode analysis was performed on both optimized geometries of ground state

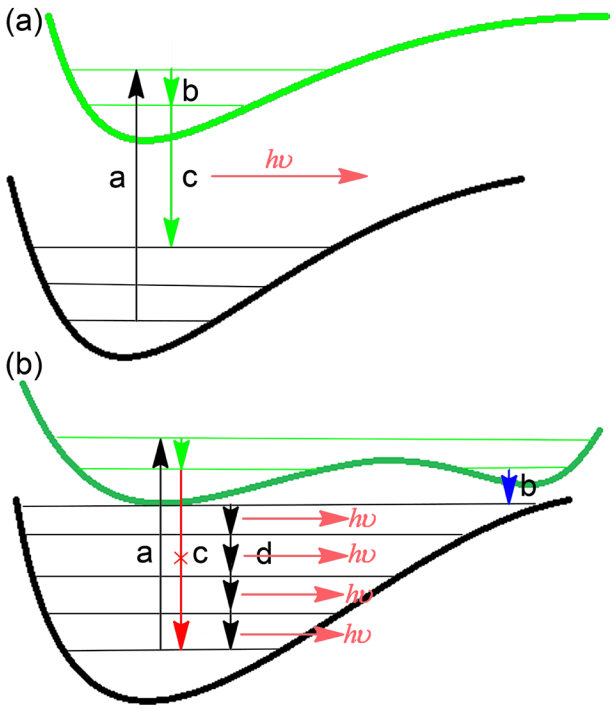

Fig. 4. Work mechanism in (a) general OLEDs and (b) electrical-driven T-rays source. In general OLED, exciton is produced by charge injection, then relaxes to a stable structure and emit by the electronic transition. In T-rays organic diode emitter: the excited state is still produced by charge injection. However, the exciton cannot transit to the ground state by direct electronic transition as this progress is optical forbidden, owing to the H-aggregation in pentacene film. The exciton can transit to the ground state by electron–phonon coupling and then emit the T-rays by the vibrational transition.

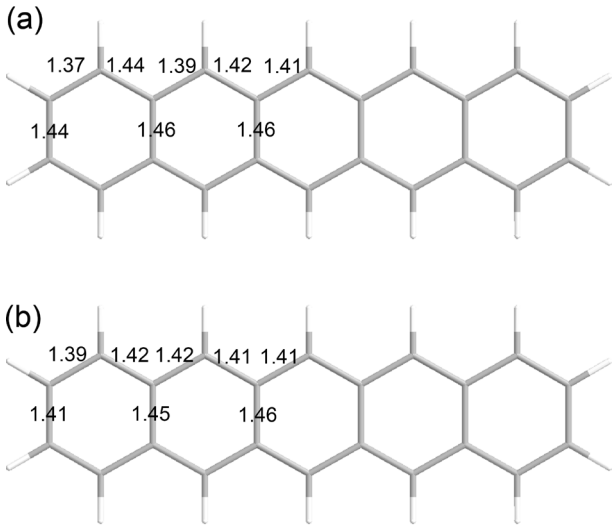

Fig. 5. Optimal structure of pentacene (a) ground state and (b) excited state.

and excited state, and further to make sure there is no virtual frequency (Fig. 5). The calculated frequencies were scaled down by the usual factor 0.9613, which has been shown to reproduce the experimental frequencies very well (Fig. 6).

The Huang–Rhys factors are evaluated through the DUSHIN program developed by Reimers[25,26].

$$\lambda_i = \sum_i \frac{1}{2} k_i \Delta Q_i^2 = \sum_i \hbar\omega_i S_i, \tag{1}$$

$$S_i = \lambda_i / \hbar\omega_i, \tag{2}$$

where λ_i is the vibrational mode resolution of total reorganization energy, ΔQ_i represents the rigid

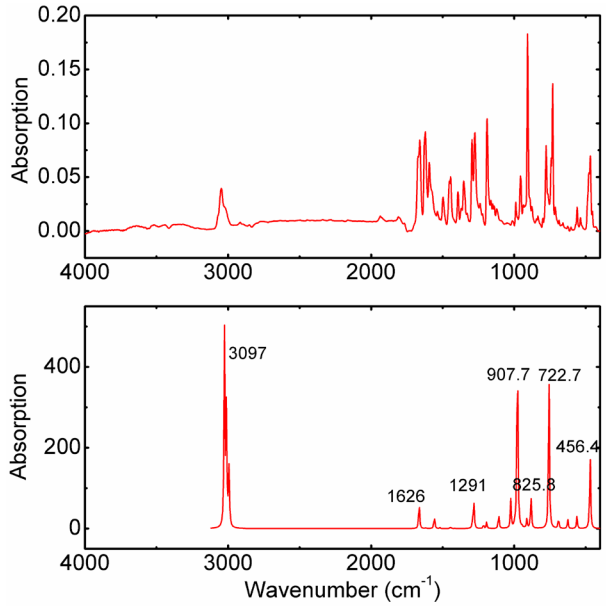

Fig. 6. IR spectrum of pentacene, the pentacene powder was dissolved in spectroscopically pure KBr. Experiment result (top), and calculation by DFT at basis set of 6–31 G (bottom).

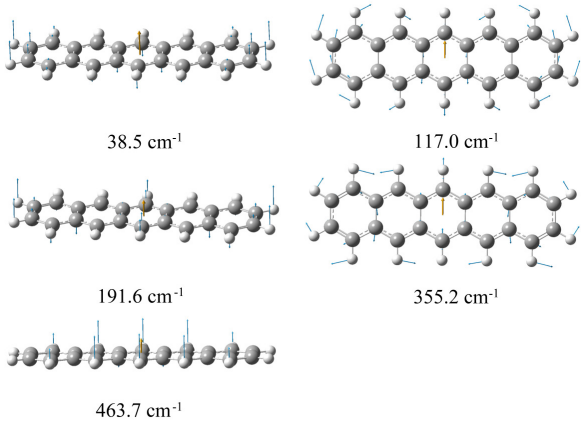

Fig. 7. Vibration models of pentacene in the terahertz zone.

displacement along the ith normal mode between the equilibrium geometries of ground-state and excited-state. k_i and ω_i are the corresponding force constant and the circular frequency for the ith normal mode, respectively, and S_i is the Huang–Rhys factor for the corresponding frequency mode. Figure 7 shows the low-frequency skeleton vibration modes of pentacene present dominant electron–phonon couplings. According to

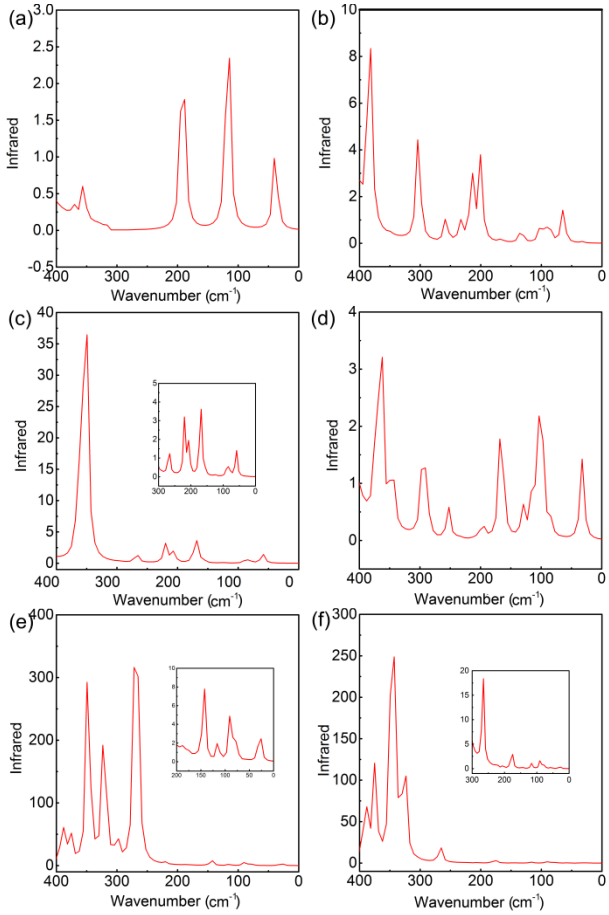

Fig. 8. IR intensity of (a) pentacene, (b) 2-fluoropentacene, (c) 2-chloropentacene, (d) 2-methylpentacene, (e) pentacene-2-amine, and (f) pentacene-2-ol in the T-ray zone.

the calculation, the strongest vibration peak in T-rays region is located at 117 cm^{-1}, which is IR active and comes from the skeleton vibration of pentacene. However, the Huang–Rhys factor in this frequency is very weak. The maximum Huang–Rhys factor is located at 257 cm^{-1}, which is an IR forbidden transition. Considering pentacene is a highly symmetrical molecule with the space group of D_{2d}, the high symmetry limits its IR activity and the strength of Huang–Rhys factor. From the relationship between reduced mass and frequency, molecule with heavier group can shift the vibration models to lower frequency, which can also introduce more useful models in T-rays region. In the following calculation, some derivatives of pentacene including 2-fluoropentacene, 2-chloropentacene, 2-methylpentacene, pentacene-2-amine, and pentacene-2-ol were chosen to explore the effect of breaking the symmetry and introducing the dipole moment to the Huang–Rhys factor. Comparing with pentacene, all the derivatives have been improved in IR activity, whereas the peaks shift to a lower frequency (Fig. 8). The Huang–Rhys factors of derivatives are shown in Fig. 9. We found that the IR and Huang–Rhys strength of all vibration frequencies of the derivatives are more than 100 times higher than those in pentacene molecule, indicating that electron–phonon coupling is strongly dependent on molecular symmetry. In 2-chloropentacene, three main frequencies in T-rays region, 228, 177, and 92 cm^{-1} are observed, and they all show relatively large Huang–Rhys factor and IR activity. We can find that pentacene-2-ol has higher reduced mass but lower Huang–Rhys factor; the same awkward situation can be found in 2-fluoropentacene and 2-chloropentacene. The result demonstrates that molecule with low symmetry is propitious to high electron–phonon coupling as well as high T-rays radiation.

However, from Eq. (2), the molecular symmetry has nothing to do with the Huang–Rhys factor, and it is influenced by force constant and the circular frequency which are corresponding to the chemical bond strength and reduced force. We therefore performed the natural bond orbital (NBO) of the pentacene and its derivatives using DFT with B3LYP hybrid functional at the basis set level of 6–31 G[27–35]. The results of NBO calculation of them are shown in Fig. 10. The Wiberg bond indices of most atoms in pentacene-2-amine are slightly higher than those in methylpentacene and pentacene-2-ol, except for the atom that the substitute is attached to. On the other hand, the reduced masses of the substituents of methylpentacene, pentacene-2-amine, and pentacene-2-ol are 0.48, 0.48, and 0.94, respectively, indicating that the skeleton strength changes induced by the substituents' dipole and conjugation may have more significant influence on the Huang–Rhys factor. For 2-fluoropentacene and 2-chloropentacene, the same trend is found from the NBO analysis. So in order to improve strength of

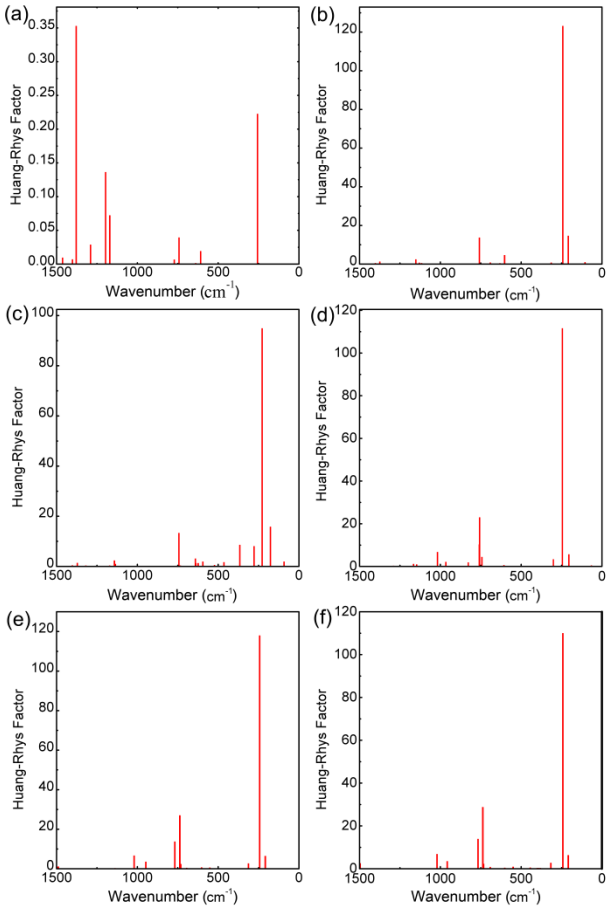

Fig. 9. Huang–Rhys factor of (a) pentacene, (b) 2-fluoropentacene, (c) 2-chloropentacene, (d) 2-methylpentacene, (e) pentacene-2-amine, and (f) pentacene-2-ol.

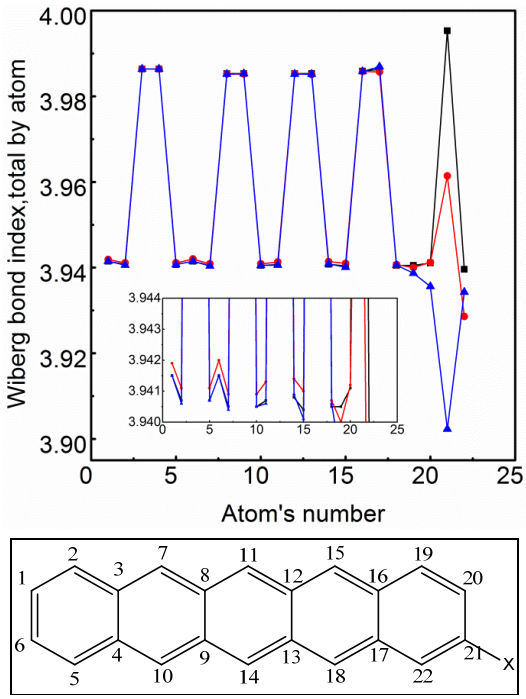

Fig. 10. Wiberg bond indices of methylpentacene (black), pentacene-2-amine (red), and pentacene-2-ol (blue), total by atom.

T-rays in organic diode-like device, further work should be concentrated on materials with good semiconducting property and asymmetric molecular structures, and more substituents can be taken into consideration.

From the above analysis, we deduce that the T-rays detected in our experiment may come from the skeleton vibration of pentacene localized at 117 cm^{-1}. However, the experiment result (78.6 cm^{-1}) and calculated result do not match very well. One possible reason is due to the difference of electronic structure of pentacene between single molecule state (theoretical calculation) and aggregate state (experiments), and some molecular vibration models might be changed or suppressed as pentacene in solid.

In conclusion, by using the process of electron–phonon coupling, the T-rays can be easily obtained. This may provide a simple and promising way to produce T-rays at room temperature. In this letter, T-rays are observed from a single-layer organic diode made with pentacene at room temperature. This work opens a new vista in the research of T-rays sources and these compact devices broaden the application of T-rays. In ongoing research, efforts will focus on the improvement of electricity-driven T-rays intensity, the active materials with strong electron–phonon coupling, high IR activity, and proper vibrational modes localized at T-rays region, and perfect properties of semiconductor should be chosen.

This work was supported by the National Science Foundation of China (Nos. 51103054 and 91233113), the Ministry of Science and Technology of China (No. 2013CB834705), and the PCSIRT (No. 20921003).

References

1. G. Niehues, A. L. Kaledin, J. M. Bowman, and M. Havenith, J. Phys. Chem. B **116,** 10020 (2012).
2. L. Zhang, N. Karpowicz, C. Zhang, Y. Zhao, and X. Zhang, Opt. Commun. **281,** 1473 (2008).
3. H. Ye, Z. Gao, Z. Qin, and Q. Wang, Chin. Opt. Lett. **11,** 031702 (2013).
4. C. Lin, I. Ho, and X. Zhang, Chin. Opt. Lett. **10,** 043001 (2012).
5. Z. Zheng, S. Lu, Y. Li, L. Chen, and S. Wen, Chin. Opt. Lett. **10,** 100605 (2012).
6. T. Nagatsuma, H. Nishii, and T. Ikeo, Photon. Res. **2,** B64 (2014).
7. X. H. Yuan, Y. Fang, D. C. Carroll, D. A. MacLellan, F. Du, N. Booth, M. Burza, M. Chen, R. J. Gray, Y. F. Jin, Y. T. Li, Y. Liu, D. Neely, H. Powell, G. Scott, C. G. Wahlstrom, J. Zhang, P. McKenna, and Z. M. Sheng, High Power Laser Sci. Eng. **2,** 1 (2014).
8. J. B. Baxter and G. W. Guglietta, Anal. Chem. **83,** 4342 (2011).
9. W. Shi, J. Xu, and X. Zhang, Chin. Opt. Lett. **1,** 308 (2003).
10. L. F. L. Costa, J. C. S. Moraes, F. C. Cruz, R. C. Viscovini, and D. Pereira, Appl. Phys. B **86,** 703 (2006).
11. R. C. Viscovini, J. C. S. Moraes, L. F. L. Costa, F. C. Cruz, and D. Pereira, Appl. Phys. B **91,** 517 (2008).
12. H. Luo, S. R. Laframboise, Z. R. Wasilewski, G. C. Aers, H. C. Liu, and J. C. Cao, Appl. Phys. Lett. **90,** 041112 (2007).
13. S. Kumar, Q. Hu, and J. L. Reno, Appl. Phys. Lett. **94,** 131105 (2009).
14. H. Fleischer and D. C. McKean, J. Phys. Chem. A **103,** 727 (1999).
15. C. M. Deng, Y. L. Niu, Q. Peng, A. J. Qin, Z. G. Shuai, and B. Z. Tang, J. Chem. Phys. **135,** 014304 (2011).
16. Y. B. Lei, S. A. Yuan, Y. S. Dou, Y. B. Wang, and Z. Y. Wen, J. Phys. Chem. A **112,** 8497 (2008).
17. Q. Peng, Y. P. Yi, Z. G. Shuai, and J. S. Shao, J. Am. Chem. Soc. **129,** 9333 (2007).
18. F. C. Spano and S. Siddiqui, Chem. Phys. Lett. **314,** 481 (1999).
19. M. Paillard, X. Marie, P. Renucci, T. Amand, A. Jbeli, and J. Gérard, Phys. Rev. Lett. **86,** 1634 (2001).
20. O. D. Jurchescu, J. Baas, and T. T. M. Palstra, Appl. Phys. Lett. **84,** 3061 (2004).
21. A. Afzali, C. D. Dimitrakopoulos, and T. L. Breen, J. Am. Chem. Soc. **124,** 8812 (2002).
22. T. Yasuda, T. Goto, K. Fujita, and T. Tsutsui, Appl. Phys. Lett. **85,** 2098 (2004).
23. D. Grischkowsky, S. Keiding, M. V. Exter, and C. Fattinger, J. Opt. Soc. Am. B **7,** 2006 (1990).
24. Gaussian 09 Version D.01, Gaussian, Inc., Wallingford, CT (2009).
25. P. Weber and J. R. Reimers, J. Phys. Chem. A **103,** 9830 (1999).
26. J. R. Reimers, J. Chem. Phys. **115,** 9103 (2001).
27. NBO Version 3.1 by E. D. Glendening, A. E. Reed, J. E. Carpenter, F. Weinhold.
28. J. P. Foster and F. Weinhold, J. Am. Chem. Soc. **102,** 7211 (1980).
29. A. E. Reed, L. A. Curtiss, and F. Weinhold, Chem. Rev. **88,** 899 (1988).
30. J. E. Carpenter, "Extension of lewis structure concepts to open-shell and excited-state molecular species," PhD. Thesis (University of Wisconsin, 1987).
31. A. E. Reed and F. Weinhold, J. Chem. Phys. **83,** 1736 (1985).
32. A. E. Reed, R. B. Weinstock, and F. Weinhold, J. Chem. Phys. **83,** 735 (1985).
33. A. E. Reed and F. Weinhold, J. Chem. Phys. **78,** 4066 (1983).
34. D. Suresh, M. Amalanathan, S. Sebastian, D. Sajan, J. I. Hubert, V. Bena Jothy, and I. Nemec, Spectrochim. Acta A **115,** 595 (2013).
35. R. Naaman and Z. Vager, *The Structure of Small Molecules and Ions* (Plenum Press, 1988).